Article:
Wang, Z. and Madathil, S. (2021) Design of a snubber circuit for low voltage DC solid-state circuit breakers. IET Power Electronics, 14 (6). pp. 1111-1120. ISSN: 1755-4535

https://doi.org/10.1049/pel2.12092

Received: 13 November 2020 | Revised: 26 January 2021 | Accepted: 15 February 2021

IET Power Electronics

DOI: 10.1049/pel2.12092

The Institution of Engineering and Technology WILEY

ORIGINAL RESEARCH PAPER

Design of a snubber circuit for low voltage DC solid-state circuit breakers

Zhongying Wang | **Ekkanath Madathil Sankara Narayanan**

Department of Electronic and Electrical Engineering, The University of Sheffield, Sheffield, UK

Correspondence
Zhongying Wang, Department of Electronic and Electrical Engineering, The University of Sheffield, 3 Solly Street, Sheffield, S3 7HQ, UK.
Email: zwang83@sheffield.ac.uk

Abstract

Solid-state circuit breakers (SSCBs) are designed to interrupt fault currents typically several orders faster than its electromechanical counterparts. However, such an ultrafast switching operation would produce a dangerous overvoltage which might cause damages to SSCBs and other circuit elements in the system. This paper proposes a novel snubber circuit for suppressing the overvoltage. It takes the advantages of both resistor-capacitor-diode (RCD) snubbers and metal oxide varistors (MOVs). Its operating process is analysed before the proposed snubber circuit for 400V DC SSCBs is designed. Pspice simulator is employed for simulating the operating process and a prototype SSCB with the proposed snubber is built and tested in a lab-scale DC system. The results of simulation and experiment validate the effectiveness of the proposed snubber.

1 | INTRODUCTION

DC distribution networks are gaining popularity in data centres, commercial buildings and transport power systems [1–4] because in comparison to traditional AC systems, they demonstrate higher efficiency and more readiness for integrating with various local renewable power sources and ever-increasing DC electronic loads. However, one of the major issues hindering this trend is the lack of effective DC short-circuit fault protection devices. Though working well in AC power networks, conventional electromechanical circuit breakers are not suitable for DC systems because their response time is typically in the range from tens of milliseconds to hundreds of milliseconds which is far longer than the survival time of most power electronic devices (a few tens of microseconds) in DC systems.

In recent years, solid-state circuit breakers (SSCBs) have been intensely researched as promising candidates to replace mechanical circuit breakers for DC protection due to its ultrafast switching speeds [5–8]. However, such a fast switching operation would produce an unacceptably high voltage across SSCBs because of the rapid fall of fault current and small system inductance [9]. Furthermore, the large magnetic energy stored in the system inductance must be dissipated by energy absorption elements since such a huge amount of burst energy during short-circuit faults is usually far higher than what SSCBs can contain. Therefore, some effective methods must be in place to suppress the overvoltage and meanwhile absorb the energy stored in the system inductance during turn-off of SSCBs. Several approaches were reported and discussed for SSCB applications [10–13]. Generally, two topologies are commonly adopted alone or combined to serve this purpose: resistor-capacitor-diode (RCD) snubbers [14, 15]and metal oxide varistors (MOVs) [16, 17].

In this paper, to start with, the operating process of both conventional RCD snubber circuits and MOVs are reviewed and their pros and cons are discussed. In the following, a novel snubber circuit combining a RCD with a MOV is proposed and analysed before the proposed snubber for 400V DC SSCBs is designed and its components are selected. Both simulation and experimental results validate the effectiveness of the proposed snubber design. Finally, the impact factors on the response time of SSCBs are investigated and conventional RCDs, MOVs are compared with the proposed snubbers.

The main contribution of this paper is:

- Proposal of a novel hybrid snubber configuration which takes into account the advantages offered by both conventional RCD snubbers and MOVs.
- Analytical expressions describing each stage of the operating process provide guidance for the snubber design for SSCB application.

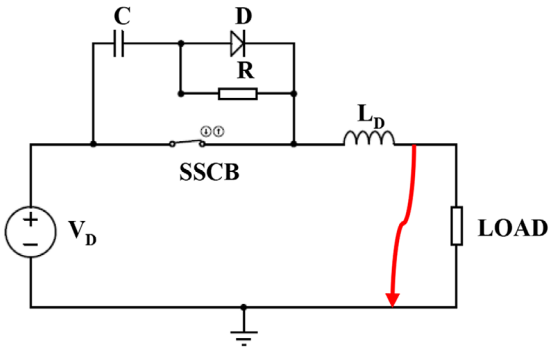

FIGURE 1 RCD snubber circuit

- The impact factors involved in the snubber on the response time of SSCBs have been identified to optimise the snubber design to meet different application requirements.

2 | REVIEW OF SNUBBER CIRCUITS FOR SSCBS

Snubber circuits in the form of capacitor(C), resistor–capacitor(RC) or resistor–capacitor–diode(RCD) have been discussed in [10, 18]. C type is the simplest. However, a high discharge current will flow through the main semiconductor switch of SSCBs during the turn-on operation, which tends to cause the nuisance trip of SSCBs. To address this issue, a current-limiting resistor is added in series to the capacitor forming RC snubbers. However, a high voltage drop across the resistor during high fault current interruption would damage semiconductor components of SSCBs. To solve this issue, a diode is added in parallel with the resistor to form an RCD snubber as shown in Figure 1.

The use of RCD snubbers has been very common for suppressing overvoltage. The operating process is simply divided into four stages as below:

Stage 1 starts when a short-circuit event occurs, the fault current ramps up until reaching the trip current level of SSCB.

Stage 2 starts when SSCB turns off and the diode D_S turns on until the fault current completely commutates from SSCB to the branch of snubber capacitor C_S and the diode D_S.

Stage 3 starts when C_S is charged until the energy stored in system inductance L_{DC} is completely transferred to C_S.

Stage 4 starts when C_S discharges through the resistor R_S until its stored energy is fully exhausted and fault current is dampened to zero.

The main advantages of the RCD snubber is very effective on slowing down the rising speed of the overvoltage and reducing the oscillations during the turn-off. However, this solution requires a very high power resistor to exhaust the stored energy in a very short period. For example, a system with $L_{DC} = 100$ μH, trip current 100 A and response time 100 μs, would require a resistor with peak power as high as 5 kW, leading to the whole snubber circuit bulky and expensive.

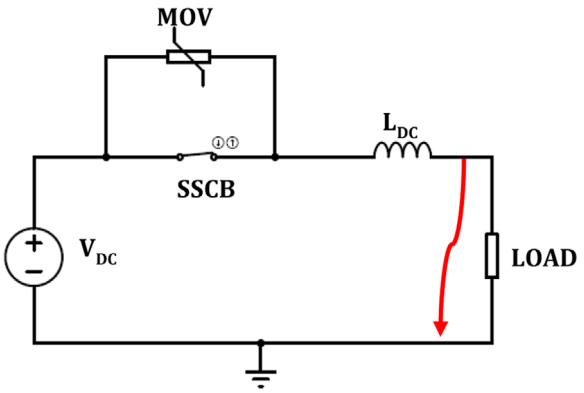

FIGURE 2 MOV snubber circuit

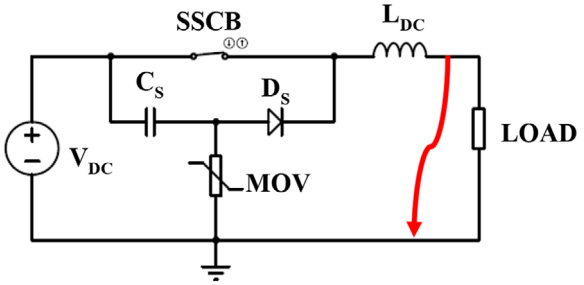

FIGURE 3 Proposed snubber circuit

MOVs are another common type of voltage clamping components which are widely used for protecting devices against overvoltage caused by either lightning surges or switching operations thanks to its highly nonlinear voltage–current characteristics like back-to-back Zener diodes.

Figure 2 shows a MOV for SSCBs application. Its operating process is divided into two stages:

Stage 1 starts when a short-circuit event occurs, the fault current rapidly ramps up to the trip current level before SSCB turns off. Once the voltage across SSCB exceeds the reference voltage of MOV, fault current starts to commutate from SSCB to MOV.

Stage 2 starts when SSCB turns off and the fault current fully commutates to MOV where the voltage across SSCB is clamped to the protection level of MOV and the energy stored in system inductance L_{DC} is dissipated until fault current is dampened to zero.

The main advantages of MOVs are its simplicity and high energy absorption capability with the typical value in the range of hundreds of joules per cubic centimetre [19]. However, it suffers from deterioration over time when frequently exposed to surges and overvoltage transients [20]. Furthermore, compared to the RCD snubber, it has no dv/dt control and displays larger transient oscillations during turn-off of SSCBs [21, 22].

To take benefits of both RCD snubbers and MOVs, a novel snubber circuit is proposed herein by combining a MOV with a RCD snubber as shown in Figure 3. This approach exploits

both effective overvoltage suppression of RCD snubbers and high energy absorption capability of MOVs. Meanwhile, it eliminates the high-power resistor of RCDs and mitigates the transient oscillations of MOVs.

3 | ANALYSIS OF OPERATING PROCESS OF THE PROPOSED SNUBBER CIRCUIT

Under normal operating conditions, SSCB stays on and the snubber capacitor is pre-charged to the supply voltage. When a short-circuit fault occurs, the operating process is divided into four stages shown in Figure 4(a)–(d) respectively. The equivalent circuit includes a SSCB, a DC supply voltage source V_{DC}, an equivalent system inductor L_{DC}, an equivalent short-circuit resistor R_{SC} and the proposed snubber circuit constructed by C_S, D_S and MOV.

To serve the main purpose of analysing the operating principle and meanwhile reducing the complexity, several assumptions are made below:

1. Ideal SSCB: turn off instantly and has zero on-resistance.
2. Ideal Diode: reverse recover characteristic is neglected.
3. MOV: Leaking current is neglected.

Stage 1: Fault current ramps up (Figure 4a)

When a short-circuit fault occurs, the fault current ramps up until it reaches the trip current I_{trip} of SSCB. At this stage, the snubber is inactive and no currents flow through C_S, D_S and MOV.

By applying Kirchhoff voltage law (KVL) to the main power circuit loop, the expression (1) is obtained:

$$V_{DC} = i_f R_{SC} + L_{DC}\frac{di_f}{dt} \tag{1}$$

Integrating the Equation (1) and rewriting it, fault current i_f at this stage can be derived as

$$i_f = I_r\, e^{-\frac{R_{SC}}{L_{DC}}t} + \frac{V_{DC}}{R_{SC}}\left(1 - e^{-\frac{R_{SC}}{L_{DC}}t}\right) \tag{2}$$

Hence, time period T_1 when fault current rise from rated load current I_r to trip current I_{trip} at this stage can be calculated as:

$$T_1 = \frac{L_{DC}}{R_{SC}}\ln\frac{I_r - \frac{V_{DC}}{R_{SC}}}{I_{trip} - \frac{V_{DC}}{R_{SC}}} \tag{3}$$

Due to the assumption of an ideal SSCB, the on-state voltage across SSCB is zero, thus:

$$V_{SSCB} = 0 \tag{4}$$

Stage 2: Fault current commutates from SSCB to the snubber capacitor C_S and D_S (Figure 4b)

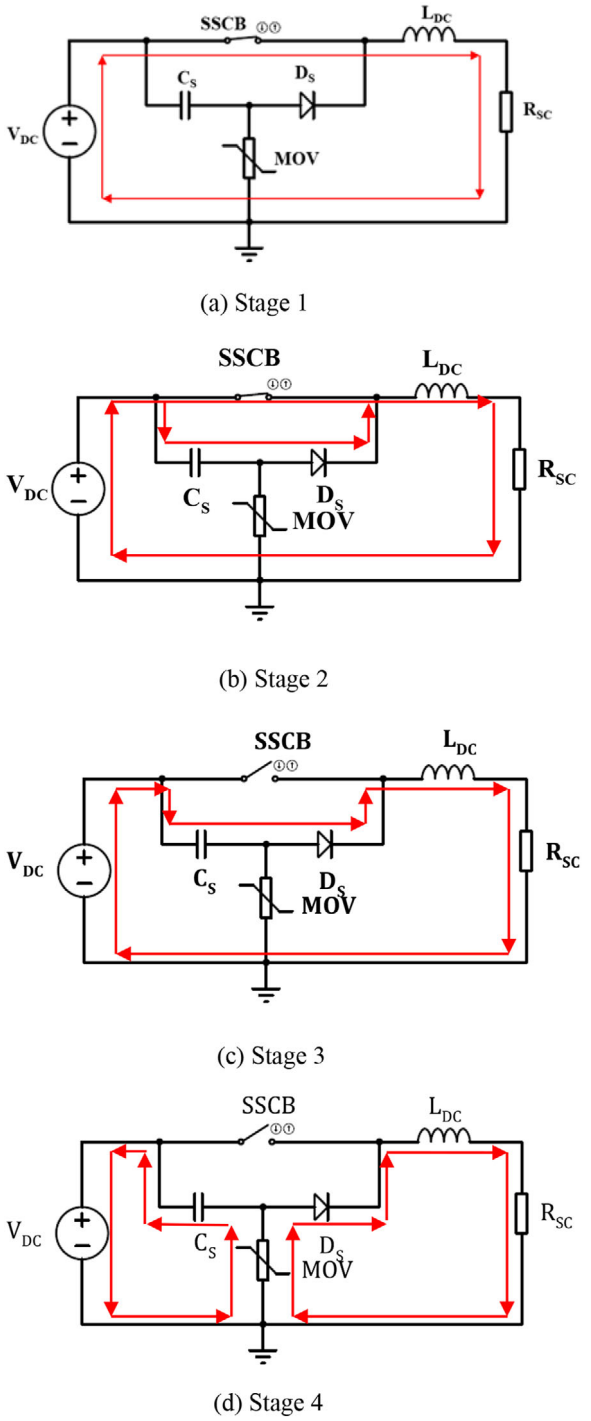

FIGURE 4 Operating process of the proposed snubber. (a) Stage 1; (b) stage 2; (c) stage 3; (d) stage 4

When SSCB starts turning off and then the snubber diode D_S turns on, the fault current is commutating from SSCB to the branch of snubber capacitor C_S and diode D_S. Again, due to the assumption of an ideal SSCB, fault current and voltage across SSCB V_{SSCB} at this stage are considered constant. Thus,

$$i_f = I_{trip} \tag{5}$$

$$V_{SSCB} = V_{DC} \tag{6}$$

$$T_2 = 0$$

Stage 3: C_S is charged until MOV is activated (Figure 4c)

The snubber capacitor C_S is charged until the voltage across MOV reaches its activated level (reference voltage V_{ref}). Fault current i_f and V_{SSCB} at this stage can be derived as

$$i_f = I_{trip}\, e^{-\alpha_1 (t - T_1 - T_2)} \cos\left(\sqrt{w_1^2 - \alpha_1^2}(t - T_1 - T_2)\right) \tag{7}$$

$$V_{SSCB} = V_{DC} + \frac{I_{trip} e^{-\alpha_1 (t - T_1 - T_2)}}{C_s \sqrt{w_1^2 - \alpha_1^2}} \sin\left(\sqrt{w_1^2 - \alpha_1^2}\,(t - T_1 - T_2)\right) \tag{8}$$

where $\alpha_1 = \frac{R_{SC}}{2L_{DC}}$, $w_1 = \frac{1}{\sqrt{L_{DC} C_s}}$

Time period T_3 at this stage can be obtained as

$$T_3 = \frac{\sin^{-1} \frac{V_{ref} C_s w_1}{I_{trip}}}{w_1} \tag{9}$$

Stage 4: Fault current commutates from the branch of C_S and D_S to MOV (Figure 4d)

MOV is activated and fault current is redirected from C_S and D_S to MOV where stored energy in L_{DC} and C_S is dissipated.

For simplicity, the V–I characteristic of MOV in its active region is assumed to be linear. Thus, V–I relationship of MOV can be simply expressed as:

$$V_{MOV} = V_A + R_B I_{MOV} \tag{10}$$

Where V_A and R_B are constant.

The initial activated current of MOV I_o can be estimated as

$$I_O = e^{-\alpha_1 T_3} \sqrt{I_{trip}^2 - (V_A C_s w_1)^2} = e^{-\frac{R_{SC}}{2L_{DC}} T_3} \sqrt{I_{trip}^2 - \frac{C_s V_A^2}{L_{DC}}} \tag{11}$$

Hence, fault current i_f and V_{SSCB} can be obtained respectively as:

$$i_f = I_O\, e^{-\frac{R_{SC}+R_B}{L_{DC}}(t - T_1 - T_2 - T_3)} - \frac{V_A}{R_{SC} + R_B}\left(1 - e^{-\frac{R_{SC}+R_B}{L_{DC}}(t - T_1 - T_2 - T_3)}\right) \tag{12}$$

TABLE 1 Technical specification of SSCB

Parameter	Value
Rated voltage (110%) V_{DC}	440 V dc
Rated current I_r	10 A
Response time T_{res}	<55 μs
Interruption current I_{trip}	<100 A
Prospective fault current	>1 kA
System inductance L_{DC}	1–100 μH
Blocking voltage $V_{B(SSCB)}$	<1000 V

$$V_{SSCB} = V_{DC} + V_A + R_B I_O e^{-\frac{R_{SC}+R_B}{L_{DC}}(t - T_1 - T_2 - T_3)} - \frac{V_A R_B}{R_{SC} + R_B}\left(1 - e^{-\frac{R_{SC}+R_B}{L_{DC}}(t - T_1 - T_2 - T_3)}\right) \tag{13}$$

Time period T_4 is estimated as

$$T_4 = \frac{L_{DC}}{R_{SC} + R_B} \ln\left(1 + \frac{I_O (R_{SC} + R_B)}{V_A}\right) \tag{14}$$

4 | SNUBBER DESIGN FOR LOW VOLTAGE DC SSCBS APPLICATION

Table 1 lists the main technical specification of the targeted low voltage DC SSCB for a 400 V DC system.

4.1 | Selection of snubber components

4.1.1 | Selection of capacitor C_S

First condition: The energy stored in C_S must be greater than the energy stored in system inductance L_{DC}. Thus:

$$\frac{1}{2} C_S \left(V_{B(SSCB)} - V_{DC}\right)^2 \geq \frac{1}{2} L_{DC} I_{trip}^2 \tag{15}$$

$$C_S \geq \frac{L_{DC} I_{trip}^2}{\left(V_{B(SSCB)} - V_{DC}\right)^2} = 3\,\mu F \tag{16}$$

Second condition: Rated voltage of C_S must be higher than the maximum blocking voltage across SSCB (1000 V).

Hence, 3 μF, 1.2 kV film capacitor B32774X1305K000 from TDK [23] is selected.

4.1.2 | Selection of diode D_S

First of all, a soft and fast recovery power diode is expected. Secondly, pulse current of D_S must be higher than the maximum trip current (100 A).

TABLE 2 Calculated results in each stage

Stage	Fault current i_f (A)	Voltage $V_{B(SSCB)}$ (V)	Time period T (μs)
Stage 1	$i_f = 1100 - 1090e^{-0.004t}$	$V_{B(SSCB)} = 0$	$T_1 = 21.5\,\mu s$
Stage 2	$i_f = 100$ A	$V_{B(SSCB)} = 440$ V	$T_2 = 0$
Stage 3	$i_f = 100e^{-0.002(t-21.5)} \cos \frac{(t-21.5)}{17.3}$	$V_{SSCB} = 440 + 577e^{-0.002(t-21.5)} \sin \frac{(t-21.5)}{17.3}$	$T_3 = 13.2\,\mu s$
Stage 4	$i_f = 770e^{-0.0056(t-34.7)} - 696$	$V_{SSCB} = 602 + 267e^{-0.0096(t-34.7)}$	$T_4 = 18\,\mu s$
Summary	$i_{f(max)} = 100$ A	$V_{SSCB(max)} = V_{DC} + V_A + \frac{V_A R_B}{R_{SC}+R_B} = 869$ V	$T_{res} = 52.7\,\mu s$

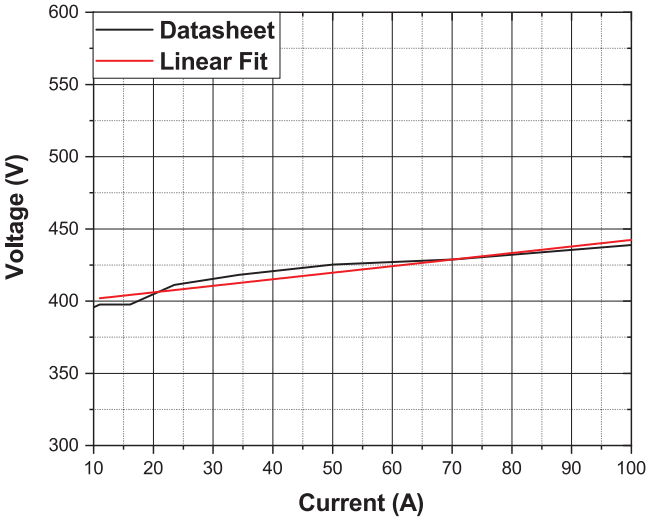

FIGURE 5 MOV V–I characteristic and its linear fitted curve

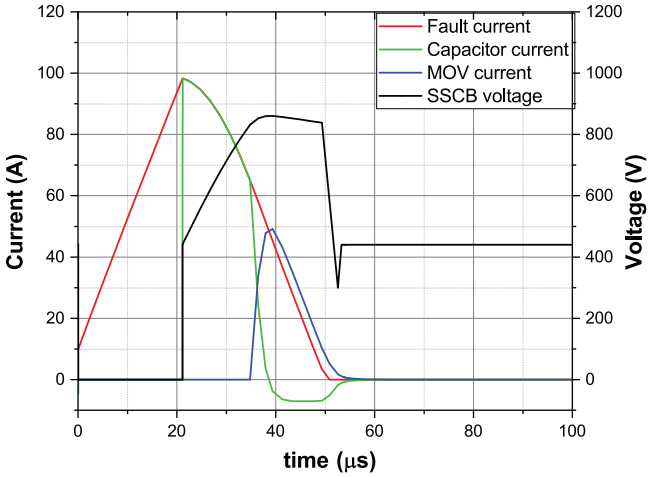

FIGURE 6 Simulation waveforms

Hence, 120 A pulse current, 650 V diode IDP40E65D2 from Infineon [24] is selected.

4.1.3 | Selection of MOV

First condition: the energy absorption capability of MOV must be higher than the energy stored in the system inductance ($L_{DC} = 100\mu$H). Thus,

$$E_{MOV} > \frac{1}{2} L_{DC} I_{trip}^2 = 0.5 \text{ J} \tag{17}$$

Second condition: the protection level of MOV must be lower than a certain level to assure the voltage across SSCB below allowed maximum value (1000 V). Thus,

$$V_{res(MOV)} \leq V_{B(SSCB)} - V_{DC} = 560 \text{ V} \tag{18}$$

Hence, MOV B72220S0171K101 from TDK [25] is selected.

Figure 5 illustrates the selected MOV voltage-current characteristic against its linear fitted curve in the active current region (10–100 A). Hence:

$$V_{MOV} = 390 + 0.56I \ (V_A = 390 \text{ V}, R_B = 0.56) \tag{19}$$

4.2 | Theoretic calculations in each stage for the proposed snubber

Substituting those parameters of selected components into corresponding equations derived in Section 3 and assuming worst scenario $L_{DC} = 100\mu$H and short-circuit resistance $R_{SC} = 0.4\Omega$, fault current i_f, voltage across SSCB $V_{B(SSCB)}$ and time period T in each stage can be calculated in Table 2.

5 | SIMULATION VALIDATION

Pspice is employed for simulating the snubber operating process. All parameters used for simulation are identical to the aforementioned theoretic calculations and an ideal semiconductor switch model is selected as SSCB.

Figure 6 shows the simulation waveforms including fault current (red line), capacitor current (green line), MOV current (blue line) and voltage across SSCB (black line). As can be seen, SSCB turns off right after fault current reaches 100 A. In the following, fault current is redirected to the snubber capacitor C_S then to MOV where it eventually damps to zero. Meanwhile, the voltage across SSCB starts rising after turn-off of SSCB until it reaches the peak value around 870 V the moment MOV is activated. In the end, the voltage converges to the steady supply voltage V_{DC} (440 V) when fault current is cleared off at around 53 μs. The simulation results confirm the proposed snubber can

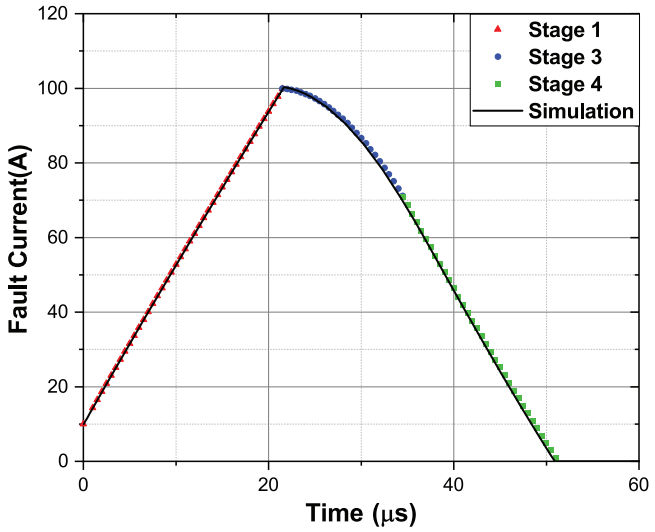

FIGURE 7 Comparison of simulated and calculated fault current in each stage

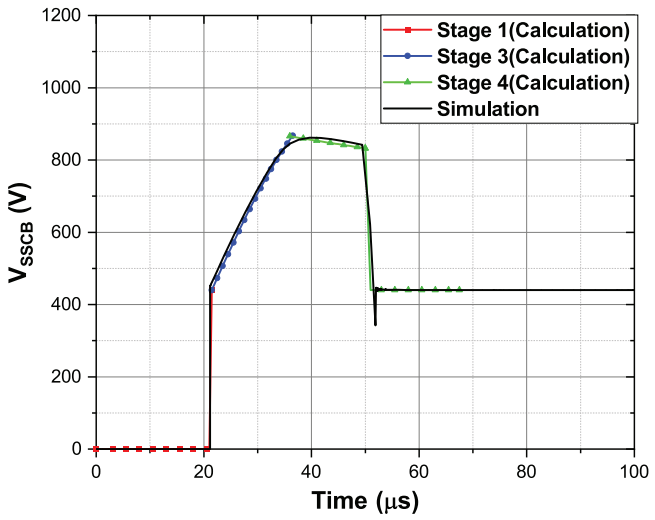

FIGURE 8 Comparison of simulated and calculated voltage across SSCB in each stage

suppress the surge voltage below 1000 V while keeping the total response time within 55 μs.

Furthermore, the analytical results for fault currents in each stage obtained from Table 2 are compared with simulation. As demonstrated in Figure 7, the analytical results match simulation very well. Furthermore, analytical results of the voltage across SSCB are also compared with simulation results in Figure 8. As can be seen, the simulation results show reasonable matching with calculated results except for some discrepancies during transient period between each stage due to the assumption involved in ideal SSCB and linear I–V relationship of MOV in the calculations. The simulation results verify the correctness of the theoretic analysis.

TABLE 3 Parameters of each component of test bench

Parameter	Value
Supply voltage V_{DC}	100–250V
Trip current I_{trip}	10–30A
Snubber capacitance C_S	3 μF B32774X1305K000 [23]
Snubber diode D_S	IDP40E65D2 [24]
MOV	B72220S0111K101 [25]
Power switch (IGBT) SSCB	IRG4PSH71UD [26]
System inductance L_{DC}	100–200 μH

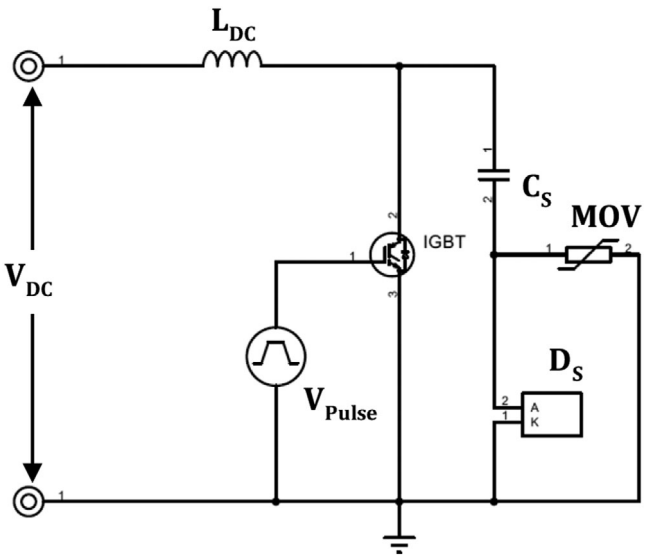

FIGURE 9 Schematic of the snubber test bench

6 | EXPERIMENT VALIDATION

The experiment of the proposed snubber circuit is conducted in a lab-scale DC system. Table 3 lists the parameters of experimental set-up. A test bench is built as sketched in Figure 9 where a power switch IGBT IRG4PSH71UD from Infineon [26] is selected as the main switch controlled by a gate driver setting the pulse duration of short-circuit current.

Figure 10 shows the experimental results of SSCB without the snubber and with the proposed snubber under the same test condition: $L_{DC} = 100$ μH and $V_{DC} = 100$ V. As observed, the peak voltage across SSCB is as high as 974 V without the snubber in Figure 10(a) compared to only 212 V with the proposed snubber in Figure 10(b).

Figure 11 presents the waveforms under the test conditions: $L_{DC} = 180$ μH subjected to various supply voltages of 150, 200 and 250 V respectively. The results demonstrate the overvoltage across SSCB can be effectively suppressed less than twice of the supply voltage with the proposed snubber. Meanwhile, it is worth noticing that in Figure 11(a), (b) voltage ringing appears at the end of the process, leading to longer recovery time of SSCB. The reason is that MOV under lower supply voltage system has not been fully activated, resulting in less dampening effect on

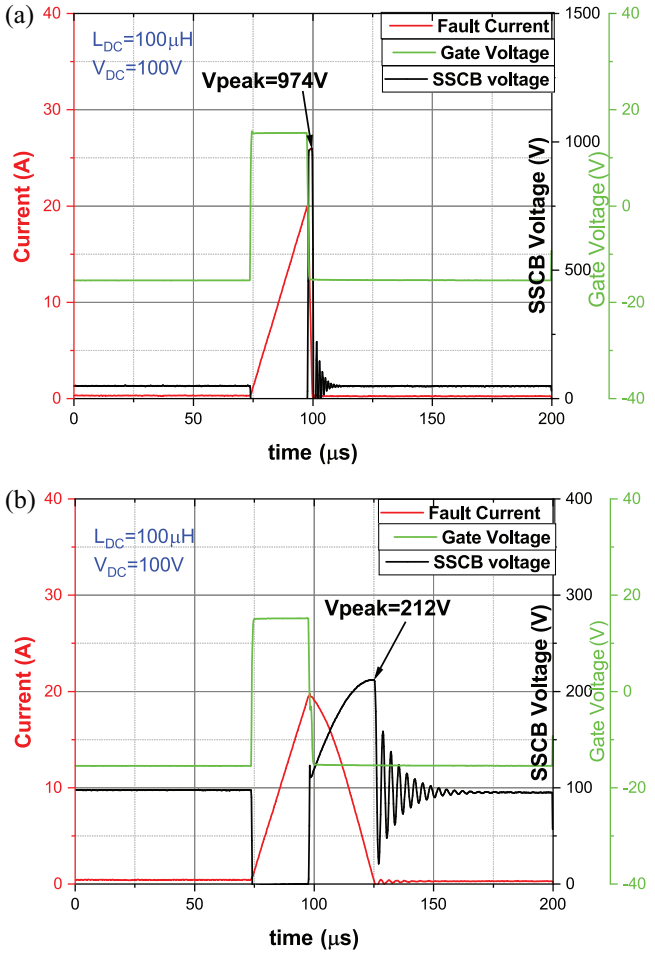

FIGURE 10 Comparison of overvoltage across SSCB (L_{DC} = 100 μH, V_{DC} = 100 V). (a) without the snubber (b) with the pr

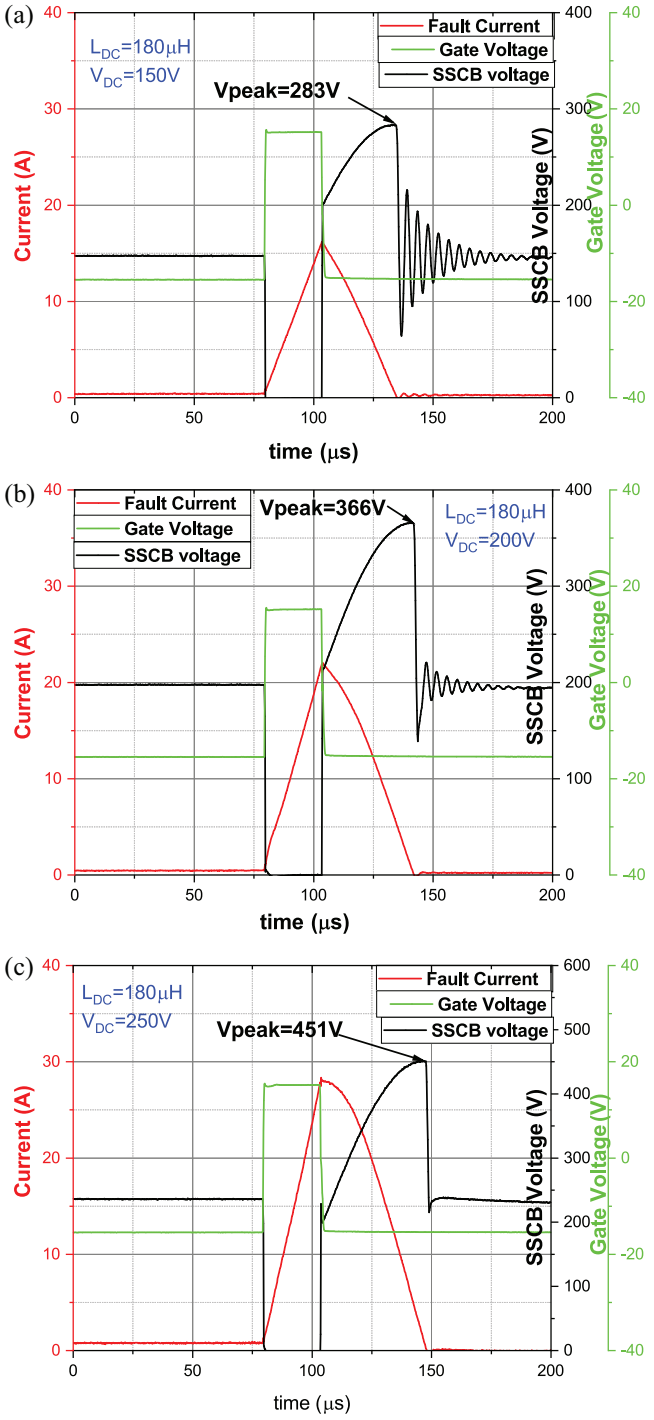

FIGURE 11 Experimental results with the proposed snubber under the condition of L_{DC} = 180 μH. (a) V_{DC} = 150V; (b) V_{DC} = 200V; (c) V_{DC} = 250V

the oscillations. In contrast, Figure 11(c) shows no ringing due to effectively activated MOV under higher supply voltage.

Figure 12 compares the waveforms of fault currents and voltages across SSCB of experiment results against simulation results under the same condition: L_{DC} = 100 μH and V_{DC} = 135 V. It demonstrates a reasonable match between them though there are noticeable discrepancies mainly attributed to the parasitic impedance of the wires and PCB traces, which are not accounted for the simulation.

In summary, the experimental results validate the effectiveness of the proposed snubber circuit.

7 | DISCUSSION

7.1 | Discussions of impact factors on the response time of SSCBs

It is well known that adoption of the snubbers can prolong the response time of SSCBs. For this reason, it is essential to investigate the factors in what way influence the response time. Figure 13 shows the simulation results of how the response time of SSCBs varies with MOV clamping voltage, snubber capacitance, system inductance and trip current respectively. As indicated, the increase of MOV clamping voltage can reduce the response time whereas the response time would increase in concert with the rising of snubber capacitance, system inductance and trip current level. Therefore, designers can manipulate these factors to meet their own design objective.

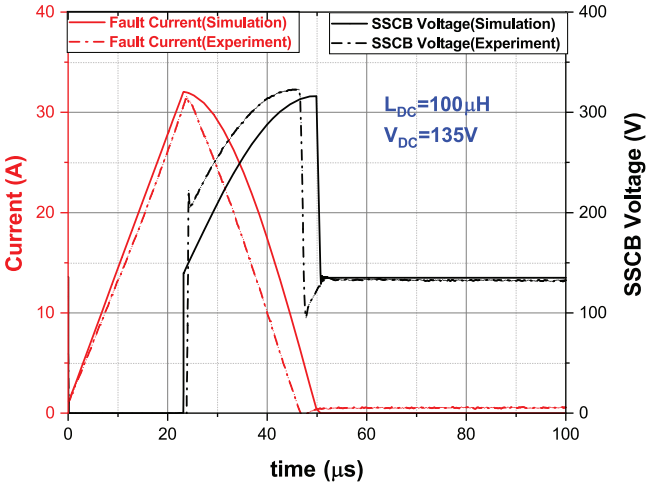

FIGURE 12 Comparison of experiment and simulation results: $L_{DC} = 100\ \mu H$, $V_{DC} = 135$ V

For convenience, the response time of SSCBs can be approximated by the equation below:

$$T_{res} = L_{DC}\, I_{trip} \frac{V_{DC} + V_A}{V_{DC} V_A} + \frac{\sqrt{C_S L_{DC}}}{2} \tag{20}$$

7.2 | Discussions of impact of the assumptions on the snubber performance

Despite a limited impact on the snubber performance due to the assumptions for simplifying the theoretic analysis, it will be discussed here for completeness.

First and foremost, the assumption of instant turn-off of SSCB tends to reduce the total response time. However, the turn-off time of semiconductor devices is generally on the order of several hundreds of nanoseconds, almost two orders lower than the total response time of SSCBs (tens of microseconds). Therefore, the influence is insignificant.

Secondly, the negligence of on-state voltage of SSCBs would increase the rising speed of fault current and tends to reduce the time period T1 in Stage 1 as defined by Equations (1) and (3). However, compared to the power supply voltage V_{DC}, the on-state voltage drop of SSCBs is negligible and hence its influence is very limited.

The assumption of no reverse current for diode D_S would have an impact on the snubber performance in the final stage where the diode is changing from a forward mode to a reverse mode. Since the diode with a slow and hard recovery characteristic would cause transient oscillations or high voltage spikes during this stage, a soft and fast recovery diode with the recovery time below 100 ns is expected. Undoubtedly, the selected diode should be verified in the actual circuit to ensure the snubber to perform as expected.

Lastly, the assumption of no leaking current of MOV has nothing influence of the snubber performance rather than MOV itself as a larger leaking current of MOVs tends to lead to the faster deterioration of MOV in the long run. In this scheme, the leaking current of MOV as a function of applied voltage is negligible as no voltage is exposed to MOV under normal operating conditions.

To conclude, if designed properly, these assumptions have little impact on the total performance of snubbers.

TABLE 4 Comparison of three snubber topologies

Parameter	RCD	MOV	Proposed snubber
Peak voltage	<900 V	<1000 V	<900 V
Peak current	100 A	100 A	100 A
Response time	<55 μs	<50 μs	<55 μs
Transient oscillations	<1% Peak voltage	<10% Peak voltage	<1% Peak voltage
Cost	£ 45	£ 0.7	£ 5

Note: Component cost calculations are based on current UK market price.

7.3 | Comparison with conventional RCD snubbers and MOVs

For comparison, a conventional RCD circuit is constructed by simply replacing the MOV of the proposed snubber with a 20 Ω snubber resistor R_S while maintaining all other parameters of the system and other components identical to the proposed snubber.

As shown in Figure 14, the simulated fault current waveforms of both solutions are almost identical. In the meantime, the peak voltage across SSCB with the proposed snubber has the same level with that of the conventional RCD snubber.

Figure 15 compares currents and powers through the resistor R_s of the RCD snubber and the MOV of the proposed snubber. As observed, both R_s and MOV experience very high peak power, 10 and 20 kW respectively. Furthermore, it is noticed that as long as 300 μs is needed to dampen the RCD snubber current to zero through the resistor R_s whereas the proposed snubber with MOV can do so by around 55 μs.

In addition, Table 4 roughly compares the performances of the conventional RCD, MOV and the proposed snubber used for 400 V DC SSCBs defined in Table 1. It shows that MOV stands out for shorter response time and a much lower cost while the conventional RCD and the proposed snubber share better overvoltage suppression and lower transient oscillations. However, RCD are much more expensive than the proposed snubber for same peak current and clamping voltage requirements.

To conclude, the comparison demonstrates that the proposed snubber cannot only suppress the overvoltage as effectively as the conventional RCD snubber but also has a relatively low cost after replacing the bulky and expensive resistor with a simple and low-cost MOV.

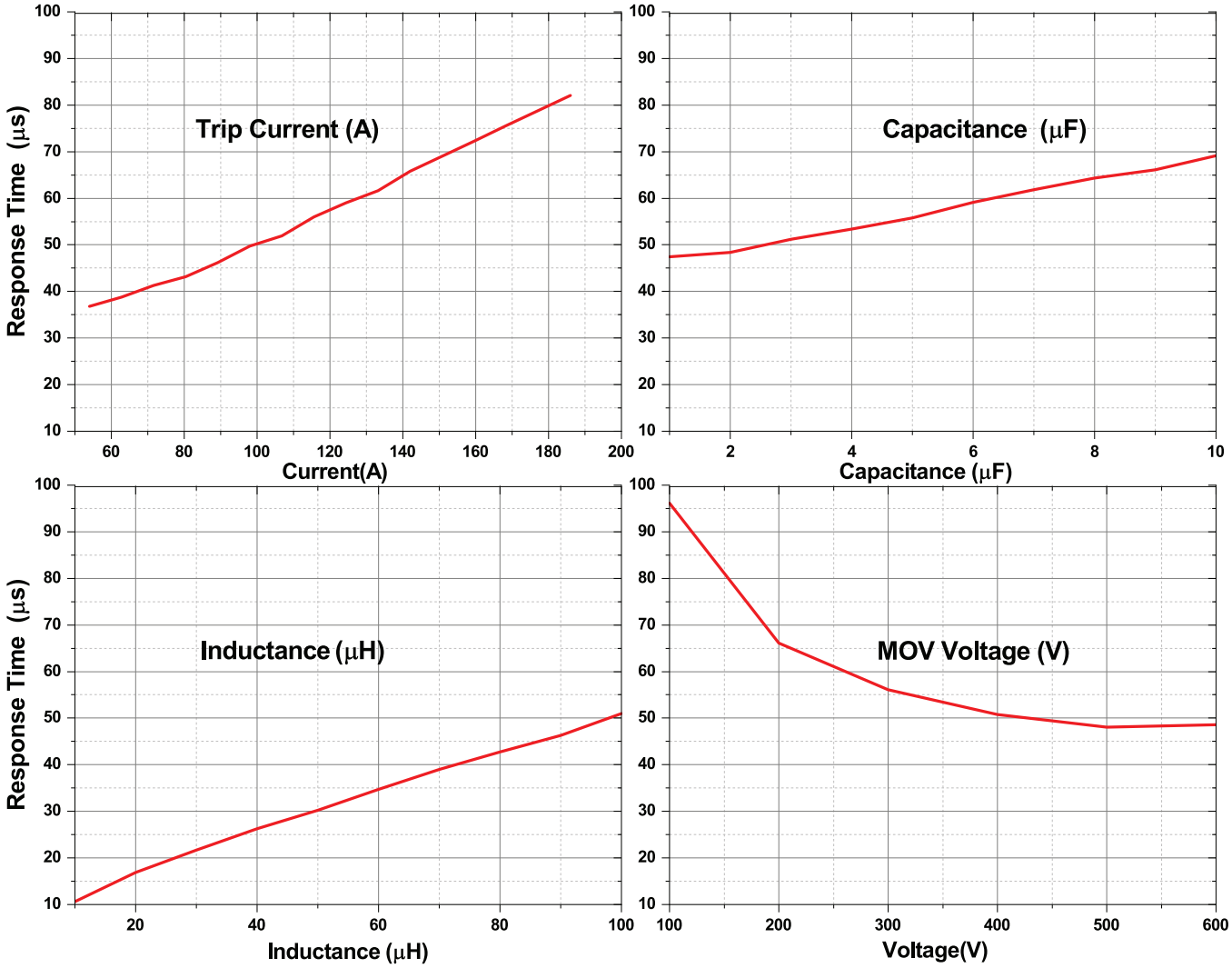

FIGURE 13 Response time as a function of trip current, snubber capacitance, system inductance and MOV clamping voltage

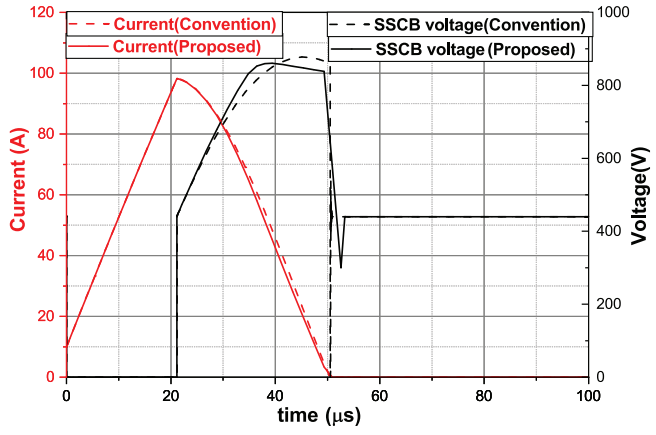

FIGURE 14 Comparison of fault current and SSCB voltage between conventional RCD and proposed snubber

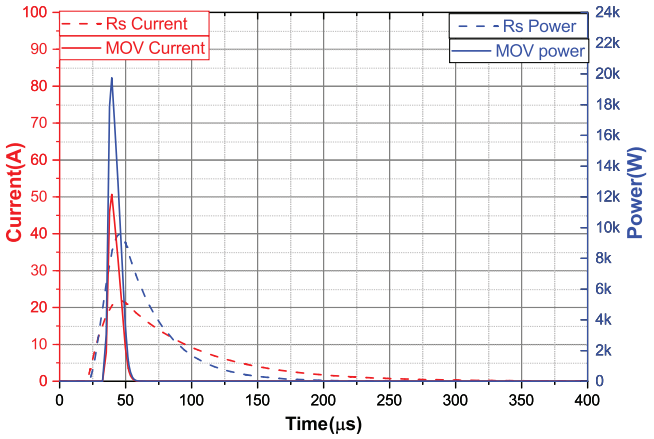

FIGURE 15 Comparison of current and power through R_s and MOV

8 | CONCLUSION

In this paper, a novel snubber circuit has been proposed for low voltage DC solid-state circuit breakers. It exploits the advantages of effective overvoltage suppression of RCD snubbers and high energy absorption capability of MOVs while it eliminates the requirement of high-power resistor of RCD snubbers and mitigates the transient fluctuation of MOVs. Its operation principle has been analysed then a snubber design for 400V DC SSCBs is presented. Simulation results against the analytic results validate the correctness of the snubber design. Meanwhile, the impact factors on the response time of SSCBs have been investigated by simulation. Finally, a prototype lab-scale SSCB with the proposed snubber circuit has been constructed and tested. The experimental results further confirm the effectiveness of the proposed snubber circuit design.

ORCID

Zhongying Wang https://orcid.org/0000-0003-4600-4990

REFERENCES

1. Baran, M.E., Mahajan, N.R.: DC distribution for industrial systems: Opportunities and challenges. IEEE Trans. Ind. Appl. 39(6), 1596–1601 (2003).
2. Pratt, A., Kumar, P., Aldridge, T.V.: Evaluation of 400V DC distribution in telco and data centers to improve energy efficiency. In: *INTELEC 07 - 29th Int. Telecommunications Energy Conf.*, pp. 32–39. IEEE, Piscataway, NJ (2007)
3. Ton, M., Fortenbury, B., Tschudi, W.: DC Power for Improved Data Center Efficiency. Lawrence Berkeley National Laboratory, Berkeley, CA (2008)
4. Salomonsson, D., Sannino, A.: Low-voltage DC distribution system for commercial power systems with sensitive electronic loads. IEEE Trans. Power Deliv. 22(3), 1620–1627 (2007).
5. Schmerda, R., et al.: Shipboard Solid-State Protection: Overview and Applications. IEEE Electrif. Mag. 1(1), 32–39 (2013).
6. Agostini, F., et al.: 1MW bi-directional DC solid state circuit breaker based on air cooled reverse blocking-IGCT. In: *2015 IEEE Electric Ship Technologies Symp., ESTS 2015*, pp. 287–292. IEEE, Piscataway, NJ (2015)
7. Urciuoli, D.P., et al.: Demonstration of a 600-V, 60-A, bidirectional silicon carbide solid-state circuit breaker. In: *Conf. Proc. - IEEE Applied Power Electronics Conf. and Exposition*, pp. 354–358. IEEE, Piscataway, NJ (2011)
8. Miao, Z., et al.: A self-powered bidirectional DC solid state circuit breaker using two normally-on SiC JFETs. In: *2015 IEEE Energy Conversion Congress and Exposition, ECCE 2015*, pp. 4119–4124. IEEE, Piscataway, NJ (2015)
9. Meyer, C., Kowal, M., De Doncker, R.W.: Circuit breaker concepts for future high-power DC-applications. In: *Conference Record - IAS Annual Meeting (IEEE Industry Applications Society)*, 2, pp. 860–866. IEEE, Piscataway, NJ (2005)
10. Park, D., et al.: Overvoltage suppressing snubber circuit for solid state circuit breaker considering system inductances. In: 10th Int. Conf. Power Electron., pp. 2647–2652. IEEE, Piscataway, NJ (2019)
11. Liu, F., et al.: Solid-state circuit breaker snubber design for transient overvoltage suppression at bus fault interruption in low-voltage DC microgrid. IEEE Trans. Power Electron. 32(4), 3007–3021 (2017).
12. Magnusson, J., et al.: Separation of the energy absorption and overvoltage protection in solid-state breakers by the use of parallel varistors. IEEE Trans. Power Electron. 29(6), 2715–2722 (2014)
13. Shin, D., et al.: Snubber circuit of bidirectional solid state DC circuit breaker based on SiC MOSFET. In: 2018 IEEE Energy Convers. Congr. Expo., pp. 3674–3681. IEEE, Piscataway, NJ (2018)
14. Liu, S., Lin, H., Wang, T.: Comparative study of three different passive snubber circuits for SiC power MOSFETs. In: *Conf. Proc. - IEEE Appl. Power Electron. Conf. Expo.*, pp. 354–358. IEEE, Piscataway, NJ (2019)
15. Yi, Q., et al.: An investigation of snubber and protection circuits connections for power-electronic switch in hybrid DC circuit breaker. In: *IEEE 10th Int. Symp. Power Electron. Distrib. Gener. Syst*, pp. 43–46. IEEE, Piscataway, NJ (2019)
16. Liao, X., et al.: Solid-state: Voltage overshoot suppression for solid-state circuit breaker. IEEE Trans. Components, Packag. Manuf. Technol. 9(4), 649–660 (2019)
17. Cairoli, P., et al.: High Current Solid State Circuit Breaker for DC Shipboard Power Systems. In: *2019 IEEE Electric Ship Technologies Symp*, pp. 468–476. IEEE, Piscataway, NJ (2019)
18. McMurray, W.: Selection of snubbers and clamps to optimize the design of transistor switching converters. In: *IEEE Annual Power Electronics Specialists Conf.*, pp. 62–74. IEEE, Piscataway, NJ (2015)
19. Levinson, L.M., Philipp, H.R.: The physics of metal oxide varistors. J. Appl. Phys. 46, 1332 (1975)
20. Khanmiri, D.T., et al.: Degradation of low voltage metal oxide varistors in power supplies. In: *Conf. Proc. - IEEE Applied Power Electronics Conf. and Exposition*, pp. 2122–2126. IEEE, Piscataway, NJ (2016)
21. Zhu, F., et al.: Performance analysis of RCD and MOV snubber circuits in low-voltage DC microgrid system. In: *Conf. Proc. - IEEE Applied Power Electronics Conf. and Exposition*, pp. 1518–1521. IEEE, Piscataway, NJ (2017)
22. Martin, W.A., et al.: Investigation of low-voltage solid-state DC breaker configurations for DC microgrid applications. In: *Int. Telecommun. Energy Conf.*, pp. 1–6. IEEE, Piscataway, NJ (2016)
23. TDK: Film Capacitors, Metallized Polypropylene Film Capacitors (MKP). (2019). Accessed: August 2019. https://www.tdk-electronics.tdk.com/inf/20/20/ds/MKP_B32774XYZ_778XYZ.pdf
24. Infineon: IDP08E65D1 Data sheet Industrial Power Control. (2013). Accessed: March 31, 2014. https://www.infineon.com/dgdl/Infineon-IDP40E65D2-DS-v02_02-en.pdf?fileId=db3a30433d68e984013d6d2dcfde1b1a
25. TDK: SIOV metal oxide varistors Leaded varistors, StandarD series Series/Type: B722*. (2011). Accessed: March 2018. https://www.tdk-electronics.tdk.com/inf/70/db/var/SIOV_Leaded_StandarD.pdf
26. Infineon: IRG4PSH71UDPbF. (2004). Accessed: September 20, 2004. https://www.infineon.com/dgdl/irg4psh71udpbf.pdf?fileId=5546d462533600a401535648c1bb233d

How to cite this article: Wang Z, Sankara Narayanan EM. Design of a snubber circuit for low voltage DC solid-state circuit breakers. *IET Power Electronics*. 2021;1–10. https://doi.org/10.1049/pel2.12092